Photochemical & Photobiological Sciences (2023) 22:1–20
https://doi.org/10.1007/s43630-022-00293-1

ORIGINAL PAPERS

Modeling acute and cumulative erythemal sun exposure on vulnerable body sites during beach vacations utilizing behavior-encoded 3D body models

Alois W. Schmalwieser[1] · Matthew A. Lohr[2] · Susan M. Daly[2] · Joshua D. Williams[2]

Received: 22 March 2022 / Accepted: 16 August 2022 / Published online: 26 August 2022

Abstract
Vacationers in a high-solar-intensity beach setting put themselves at risk of ultraviolet radiation (UV) over-exposure that can lead to acute and chronic health consequences including erythema, photoaging, and skin cancer. There is a current gap in existing dosimetry work on capturing detailed time-resolved anatomical distributions of UV exposure in the beach vacation setting. In this study, a radiative transfer model of the solar conditions of Tampa Bay, St. Petersburg, Florida, USA (27.8°N, 82.8°W) is combined with an in silico three-dimensional body model and data on typical beach vacation behaviors to calculate acute and cumulative body-site-specific UV exposure risk during a beach vacation. The resulting cumulative UV exposure calculated for a typical mix of clothing choices, settings, and activities during a week-long (7-day) beach vacation is 172.2 standard erythemal doses (SED) at the forearm, which is comparable with the average total annual UV exposure of European and North American residents and consistent with existing dosimetry studies. This model further estimates that vacationers choosing to spend a full day exclusively in the beach or pool setting can experience UV exposure in excess of 50 SED a day at multiple body sites. Such exposure indicates that significant sun protective measures would be required to prevent sunburn across all skin types in this setting. This work clarifies the significant role that beach vacations play in UV exposure and corresponding acute and cumulative health risks and highlights the importance of behavioral choices (including clothing, activity and photoprotection) as crucial factors in differentiating personal solar exposure risks.

✉ Alois W. Schmalwieser
alois.schmalwieser@vetmeduni.ac.at

[1] Unit of Physiology and Biophysics, University of Veterinary Medicine, Veterinaerplatz 1, 1210 Vienna, Austria

[2] Johnson and Johnson Consumer Inc., Skillman, NJ, USA

Graphical abstract

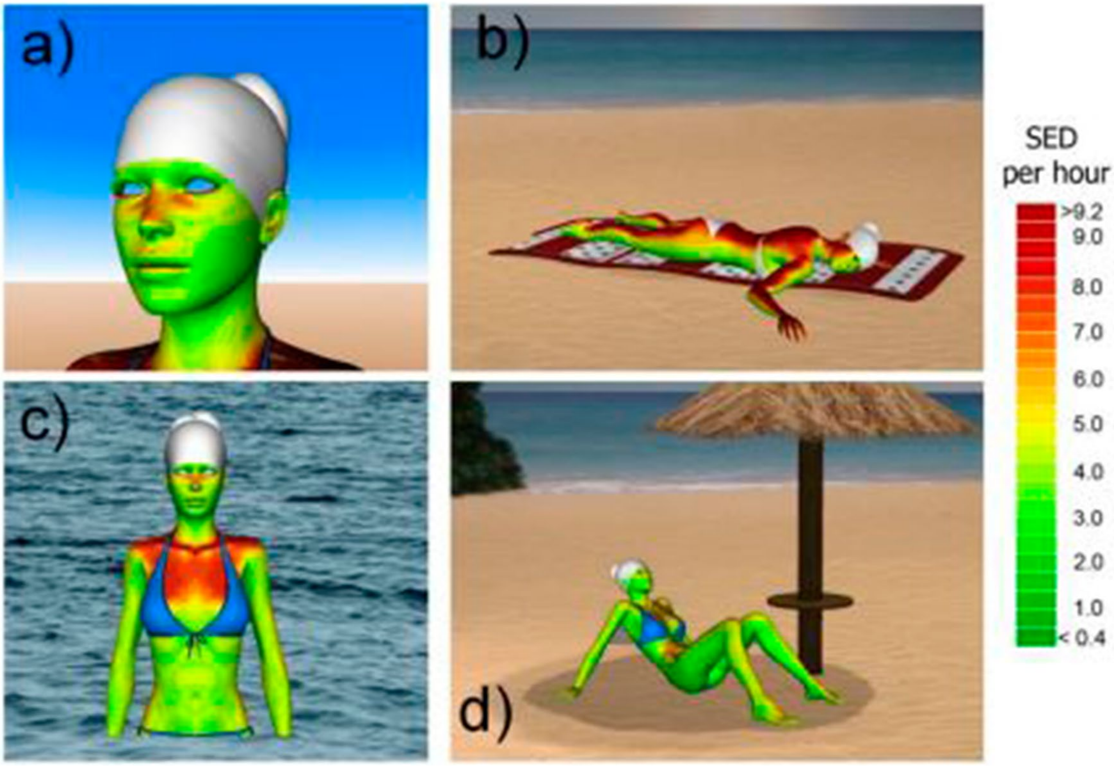

Keywords Sunburn · UV index · Beach vacation · 3D body modeling · Solar exposure · In silico

1 Introduction

Beach vacations are a common pursuit of sun-seeking tourists, and consequently a widespread source of intense intermittent solar exposure. For the year 2019, the United States Lifesaving Association identified 408 million beach attendances in the United States [1]. Over 43 million of these took place in Florida [1], where the mean ultraviolet (UV index) is 8 or higher during the spring and summer months of April to August [2]. While rest, relaxation, and aquatic recreation pursued during beach vacations can contribute to general health and well-being [3], the associated high frequency of acute ultraviolet radiation (UV) overexposure and addition to lifetime cumulative UV doses are known contributors to negative skin health outcomes, including skin cancer [4, 5].

High risk of solar overexposure and sunburn in the beach vacation setting is widely documented. Studies have specifically documented that sunburn [6] and associated cutaneous deoxyribonucleic acid (DNA) damage [7] occur more often during beach vacations or sun seeking holidays. Several investigators have shown that UV exposure received during vacations or holidays makes up a significant portion (in some estimates, 30–50%) of an individual's total annual UV exposure [4, 8–11]. Despite prevalent evidence on the connection between sunburn and skin damage/cancer, high incidences of sunburn in the beach setting persist globally [12, 13]. Beach vacations are particularly risky because they combine multiple activities associated with high sun exposure, like traveling/vacationing for leisure (associated with 20.7% of sunburn occurrence of U.S. residents) and swimming/spending time in the water (associated with 32.5% of U.S. sunburn occurrence) [14]. This indicates a continued need for impactful and compelling interventions to bring awareness to risk conditions for excessive UV exposure in hopes of mitigating both short- and long-term skin health consequences.

Tools which have been used to study solar exposure in the beach setting include an extrapolation of UV exposure from behavioural and location information acquired from surveys and personal subject diaries as well as quantitative measurements of personal UV exposure directly from worn dosimeters [9, 10, 15–17]. Direct measurements of UV exposure are restricted to body sites where a dosimeter can be worn without compromising its functionality (e.g. through prolonged water submersion or rigorous physical activity). Data resulting from these assessments are difficult to extrapolate to other body sites, other geographical exposure locations, and other seasons of the year [18].

Relevance and accessibility of learnings from direct UV exposure measurements can be enhanced through utilization of realistic in silico three-dimensional (3D) human body models. For more than a decade, body models have been used in conjunction with radiative transfer models to facilitate calculation of solar UV irradiance across body sites within specific sun exposure settings [19–21]. Model calculations have aligned well with direct measurements of personal UV exposure, generally within measurement uncertainties of (± 15%) [22]. These in silico models provide compelling visual snapshots of UV exposure patterns on human figures in specific solar conditions.

In this study, a high-resolution 3D in silico body model is utilized to calculate and visualize UV exposure doses at different body sites across a diverse assortment of settings and behaviors typical of a week-long beach vacation. By factoring in existing behavioral data on representative postures, activities, and clothing choices, the model highlights body sites subject to high levels of irradiation across various settings and estimates resulting cumulative body-site-specific erythemal weighted exposures. Combining in silico data and known local solar irradiance conditions with behavioral information creates finer time-based and spatial body-site resolution than existing in-world dosimeter type studies or computational work. This model provides further insights into the relative influences that behavior and activity choice can have on body-site-specific solar exposure within a beach vacation setting.

2 Methods

An in silico model of personal UV exposure is assembled from aggregated information on ambient UV radiation (location, date, time, cloudiness, total ozone, aerosols, and albedo), personal behavior (activities, postures, duration of exposure), and choice of clothing. For this evaluation, realistic sun-exposure environments were drawn from an exemplative beach vacation location and representative behavioral distributions were constructed based on data available from published observational studies from a high-UV index western beach vacation destination. High-resolution 3D-models with postures and attire based on representative behavioral distributions and sun exposure environments were generated and utilized to establish acute and cumulative UV exposure on various body sites.

2.1 Erythemally effective UV radiation

Radiative transfer calculations were done for the location of Tampa Bay, St. Petersburg, Florida, USA (27.8°N, 82.8°W, 0 m above sea level) for the week of 27 April–3 May, between sunrise and sunset (~ 13 h). Version 2.9.5 of the radiative transfer model Simple Model of the Atmospheric Radiative Transfer of Sunshine (SMARTS2) [23, 24] was used to calculate the direct and diffuse spectral UV irradiance falling on inclined planes of all directions (0°–360° in azimuth as well as in declination) with a step width of 5° × 5°. With these, and the field of view of the receiving surfaces (see below), the calculations mimic a radiance model (e.g. [25]) but incorporate simplifications (e.g. homogeneous sky radiance) compared to a radiance model. Calculations were done with a temporal resolution of 15 min following the course of the sun during this week. Environmental options of a cloudless sky (cloud modification factor of 1) with a sub-tropical summer atmosphere, maritime aerosols, surrounding ocean water (albedo), and dry light sand (albedo) were selected from the SMARTS2 options [see 23, 24 for details] to best model the beach vacation location of interest. Cloudless sky selection was justified by the specified week in April/May having the lowest probability for rain (< 20%) and the highest probability of predominately cloud free sky (> 50%) compared with typical weather at this location over the course of an average year [26], as well as an average daily sunshine duration of ~ 10 h [27]. A cloud modification factor of 1.0 allows for occasional light cloud coverage, as measures of cloud modification factor for fractional cloud coverage up to 25% have been shown to be within error of 1.0 [28]. Total ozone was taken from NASA's Ozone Monitoring Instrument onboard the AURA satellite and was around 287 Dobson Units (DU; 275 DU–297 DU) during this week.

Spectral irradiance per unit wavelength (λ) as a function of solar elevation (α) and azimuth (β), $E(\lambda,\alpha,\beta)$, was weighted by the erythemal action spectrum $s_{ery}(\lambda)$ as standardized by the International Commission of Illumination [29] and integrated over the wavelength range from 280 to 400 nm to yield the erythemally effective irradiance $E_{ery}(\alpha,\beta)$ in units of W/m^2 of erythemal radiation:

$$E_{ery}(\alpha,\beta) = \int_{\lambda=280nm}^{400nm} E(\lambda,\alpha,\beta) \bullet s_{ery}(\lambda) d\lambda.$$

Erythemally effective irradiance can be expressed in terms of the UV index, an internationally accepted measure used to inform the public about the intensity of the sun and to advise on relevant sun protective measures [30]. Recent local UV index values are provided by forecasts [31] and online measurements [32]. A UV index value of 1 is equivalent to 25 mW/m^2 of erythemally effective irradiance [33]. During this week (27 April–3 May), the UV Index (on a horizontally oriented surface) reaches a value of 10.9 at noon under clear sky conditions.

Erythemally effective UV radiant exposure H_{ery} is calculated by integrating irradiance $E_{ery}(\alpha, \beta)$ over the time duration of interest:

$$H_{ery}(\alpha,\beta) = \int_0^t E_{ery}(\alpha,\beta) \bullet dt,$$

H_{ery} can be expressed in units of standard erythemal dose (SED) [29], for which 1 SED is equal to 100 J/m^2 of erythemally effective radiant exposure. A UV index of 1 is equivalent to 90 J/m^2/h of erythemally effective irradiance, or 0.9 SED/h.

2.2 Sun-exposure environments during a beach vacation

Specific sun-exposure environments during beach vacations were derived from Petersen et al. [10], in which the time spent at different exposure environments over the course of a beach vacation (March, Tenerife, Canary Islands, Spain, 28°N, 16°W) were recorded by study participants in time stamped diaries. The behavioral data from Tenerife was leveraged for this model of the Tampa Bay/St. Petersburg area of Florida since the season, latitude, and climate are similar between these two locations. Over the course of an entire day of solar exposure (07:00–19:00), individuals reported spending 19% of the day at the beach, 11% at the pool, 14% on the balcony, 14% in the city, 10% in other outdoor environments, and 32% indoors. This corresponds to roughly 3.6 h spent in the beach or pool setting, 2.9 h spent in the city or other outdoor settings, and 1.7 h on a balcony during daylight hours. During hours of peak solar intensity (12:00–15:00), individuals reported spending 36% of their time at the beach, 20% at the pool, 6% on the balcony, 16% in the city, 14% in other outdoor environments, and 8% indoors. For this study, the frequency of each activity during the 07:00–12:00 and 15:00–19:00 time windows was calculated by subtracting the activity values for 12:00–15:00 from whole day activity values and distributing remaining time evenly across these time intervals.

These settings (beach, pool, city, other outdoor locations, balcony and indoors) are grouped based on extent of sky obstruction (Table 1). This factor has differentiated impacts on diffuse and direct components of solar UV radiation; while diffuse UV radiation is reduced by a set quantity throughout the day, direct UV radiation is primarily obstructed at low solar elevations in the morning and evening. For the beach and pool settings, a free or unobstructed horizon was utilized. For the city/town and other outdoor settings away from the pool or beach, a partially obstructed sky was assumed whereby the UV irradiance is reduced by 30% (according results from [17]). It was assumed that 50% of the sky was obstructed by a vertical wall in the shaded balcony setting [34]. For specific locations such measures could be gained by sophisticated methods [e.g. 35]. For time spent indoors, the sky is completely obstructed and UV exposure was set to zero.

2.3 Body models

3D-body models were prepared in silico and combined with behavioral data through incorporation of clothing and posture combinations relevant to beach vacation sun exposures. Complex anatomical features were resolved in these models as a fine mesh of polygons, with about 5000 individual polygons comprising the face alone, each with a distinct orientation with respect to the sun (Fig. 1). Each polygon had a unique identifier and was described by its corner points, a normal vector (that defined the direction away from the body), and a binary variable $\Gamma_{i,j}$ that indicated whether each polygon was covered by clothing. Polygons were grouped into body sites commonly denoted in discussions of site-specific UV exposure. For example, though areas of the ears, nose, forehead and cheeks may experience different fluxes of UV radiation, are all included in the area commonly referred to in discussions of UV exposure as the "head." Erythemally effective irradiance falling on each polygon *j* at time *t*, $E_{0,j}(t)$, was determined by the radiative transfer model described in Sect. 2.1 and the subsequent calculation of erythemally effective irradiance $E_{ery}(\alpha,\beta)$ incident perpendicular to the surface of polygon *j*.

Table 1 Time spent in different sun exposure settings during the course of a day on a beach vacation (adapted from Petersen et al. [10]) and percent of sky obstructed (see text)

Location	07:00–12:00		12:00–15:00		15:00–19:00		Total daily time	Sky obstructed
	[%]	[h]	[%]	[h]	[%]	[h]	[h]	[%]
Beach	13	0.7	36	1.1	13	0.5	3.6	0
Pool	8	0.4	20	0.6	8	0.3		
City	13	0.7	16	0.5	13	0.5	2.9	30
Outdoor	9	0.4	14	0.4	9	0.3		
Balcony	17	0.8	6	0.2	17	0.7	1.7	50
Indoor	40	2.0	8	0.2	40	1.6	3.8	100

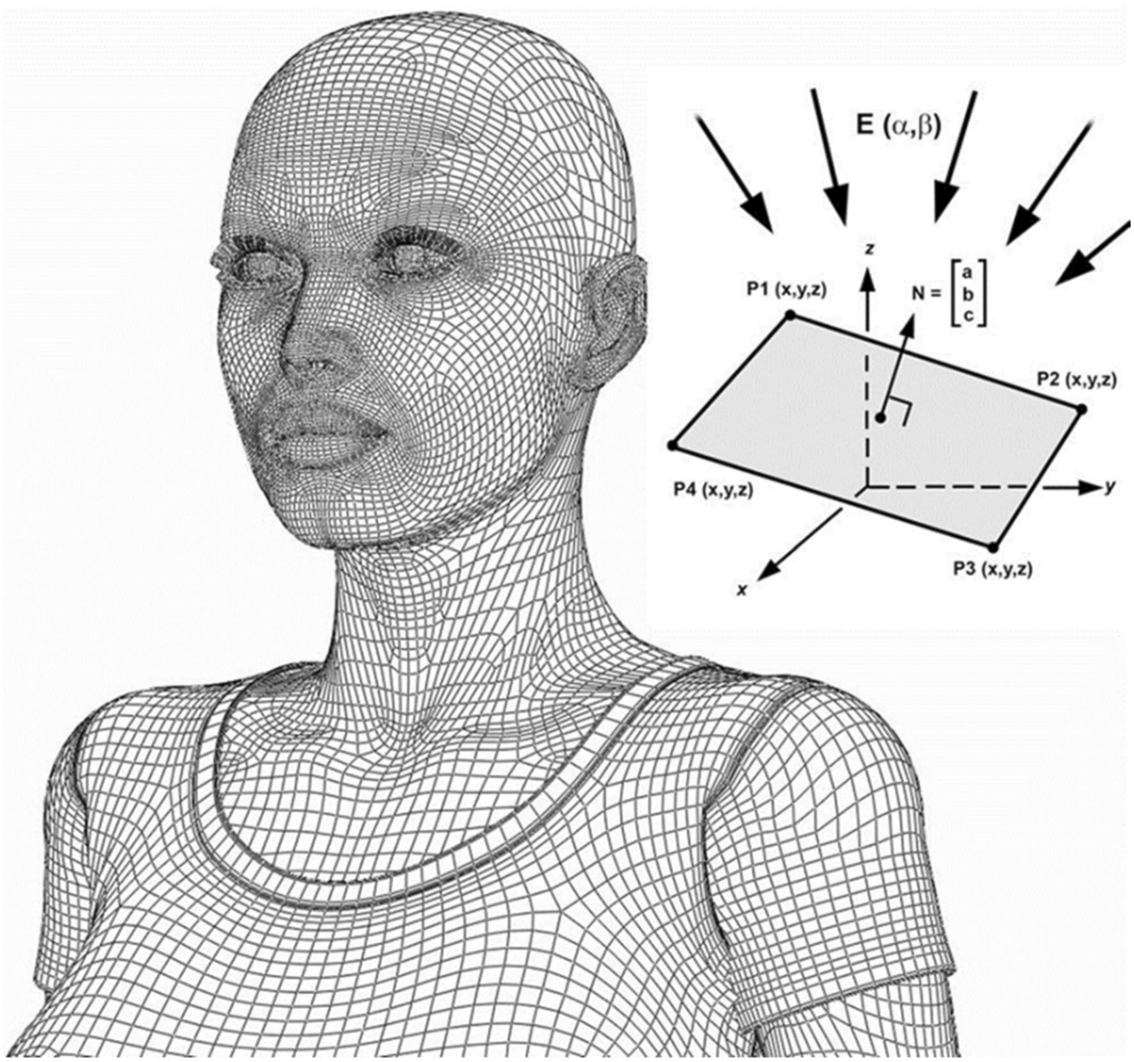

Fig. 1 Example visualization of polygon-comprised mesh surface body model. Example of a single polygon (defined in a Cartesian coordinate system with coordinates (x, y, z) by vertices P1, P2, P3 and P4) subject to irradiance E (α, β) given in upper right of figure. The polygon is subject to the component of irradiance E (α, β) parallel to the polygon's normal vector $N=[a, b, c]$

To account for UV protective coverage by specific garments, the average behavior-weighted erythemal irradiance $E_j(t)$ on a certain polygon j at time t was calculated as

$$E_j(t) = E_{0,j}(t) \bullet \sum_i \left(f_i(t) \bullet \Gamma_{i,j}\right)$$

for which for which $E_{0,j}(t)$ is the erythemally effective irradiance at polygon j at time t, $f_i(t)$ is the relative frequency of clothing choice i at time t, and $\Gamma_{i,j}$ is the coverage of polygon j by clothing choice i (either 0 or 1, as it is assumed that garments are completely protective against UV exposure).

The body model used was the Victoria 4.2 Base (Daz Productions Inc., Salt Lake City, UT, USA), an adult female figure (height: 176 cm, waist circumference: 70 cm, feet to thigh: 80 cm, wrist to shoulder: 53 cm) with short hair/hair in a bun (a hairstyle chosen to remove additional complexities imparted by shadowing). The model could be oriented in a range of postures: standing, walking, sitting (upright and reclining) and lying down (prone and supine). The body model could be covered with a range of garment options, including a bikini top, tank top, short sleeve shirt, 3/4-sleeve shirt or long sleeve shirt for the upper body, and bikini bottom/swimming trunks, short-length trousers, knee-length trousers, 3/4-length trousers or long trousers for the lower body. Examples of modelled postures and clothing combinations are illustrated in Fig. 2. In this model, clothing was treated as tight-fitting so it covers discrete polygons regardless of the angle of incidence of radiation and shading effects from clothing (e.g. loose skirts) are not considered. To best highlight local UV overexposure risk, the erythemally effective irradiance at a body site at a given hour is defined as the

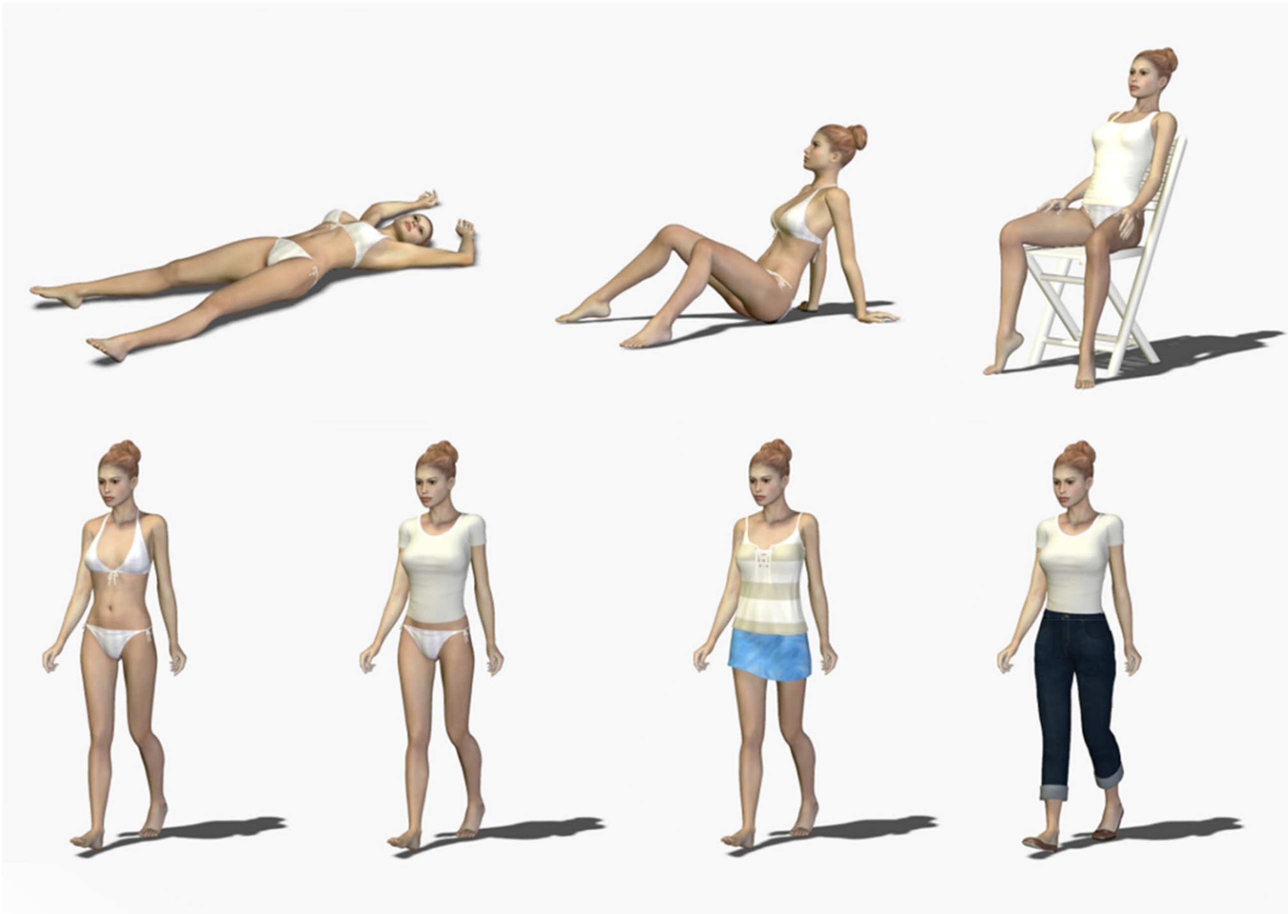

Fig. 2 Examples of modeled postures (top left to right: lying down (supine), sitting (reclining), sitting (upright) and clothing options with varying exposed body area (EBA) (bottom left to right: bikini top and bottom, total EBA = 85%; short-sleeve shirt and bikini bottom, total EBA = 51.9%; tank top and short skirt, total EBA = 54.5%; short-sleeve shirt and 3/4 length trousers, total EBA = 25.4%) utilized with 3D sun exposure models.

highest erythemally effective irradiance at a single polygon comprising that body site.

2.4 Exposed body area and clothing choices during a beach vacation

In this model, time- and location-dependent exposed body area (EBA) as well as related clothing choices in various settings during a beach vacation were defined from existing observational studies. EBA during a beach vacation has been described by Petersen et al. [10], in which clothing and location were indicated by study participants in time stamped diaries. This study found that the average EBA was 67% at the beach, 46% on the balcony, and 36% in the city, with similar average EBA's between the beach and pool and between the city and other outdoor locations. Average EBA for each sun exposure location (loc) is referred to here as EBA_{loc}, with the EBA resulting from specific choice of clothing being independent of body shape [36].

Petersen et al. [10] created a time-dependent function to describe EBA by fitting a quadratic curve to EBA estimates calculated at discrete times based on the clothing diaries of study participants. This function, which is designated here as $EBA_{all}(t)$, is given as

$$EBA_{all}(t) = -0.7337 \times t^2 + 19.552 \times t - 72.758,$$

$EBA_{all}(t)$ is lowest in the morning and evening (around 40%), and peaks between 13:00 and 14:00 above 57%. The mean value of this function between 08:00 and 19:00 is 50.05%, which is reached at about $t = 10{:}15$ and $t = 16{:}30$.

$EBA_{loc}(t)$ for each location was calculated for this work by normalizing the $EBA_{all}(t)$ function by the mean EBA_{all}, 50.05%, and then multiplying by the average EBA for each location, EBA_{loc} (e.g., at 13:00 in the beach/pool setting, $EBA_{beach}(t = 13{:}00) = 77\%$). These location-and-time dependent $EBA_{loc}(t)$ functions allowed for the definition of typical time-and-location dependent women's clothing choice prevalence for each setting. EBA values associated with each garment type as described by Petersen et al. [10] and incorporated in this model are provided in Table 2. The whole body EBA was determined by summation of EBA for the upper body (EBA_{upper}) and lower body (EBA_{lower}). For example, a body model wearing a bikini top ($EBA_{upper} = 46.5\%$) and bottom ($EBA_{lower} = 38.5\%$) exposes 85% of total body surface area. Replacing a bikini top with a tank top reduces total EBA to 65%.

An estimate of the time- (t) and location- (loc) dependent frequency distributions of each potential clothing choice covering the top (i) or bottom (j) halves of the body of vacationers, $f_{upper,loc,i}(t)$ and $f_{lower,loc,j}(t)$, respectively, is calculated such that a fit function $EBA\_fit_{loc}(t)$ is recovered that most closely matches the previously defined $EBA_{loc}(t)$:

$$EBA\_fit_{loc}(t) = \sum_{i,j} EBA_{upper,i} \times f_{upper,loc,i}(t) + EBA_{lower,j} \times f_{lower,loc,j}(t),$$

$$\Delta EBA(t) = EBA_{loc}(t) - EBA\_fit_{loc}(t) \rightarrow 0.$$

Reasonable values for $f_{upper,loc,i}(t)$ and $f_{lower,loc,j}(t)$ were assigned by making simplifications about clothing choice in these settings. Long sleeves, long trousers/long skirts, and swimming trunks were excluded as infrequent stylistic choices at all locations, given the high temperatures and stylistic trends during beach vacations. Clothing options in public settings were restricted to those most appropriate to the location and temperature (e.g. excluding bikini tops/bottoms at outdoor locations away from the beach and excluding 3/4 length shirts at the beach/pool). Further, $f_{upper,loc,i}(t)$ and $f_{lower,loc,j}(t)$ were selected so that they were uniformly continuous over time and $\Delta EBA(t) \leq 0.4\%$. From these assumptions, clothing choices were reasonably assigned that evolved continuously over the course of the day.

2.4.1 Clothing choices in the beach/pool setting

The beach or pool is characterized by the least conservative clothing choices and highest resultant EBA's of all sun-exposure settings in the beach vacation context. Calculated frequency distributions of clothing choice that provide a best fit to $EBA_{beach/pool}(t)$ can be found in Table 3. For the beach setting, a simplified selection of women's clothing options of bikini top/tank top/short sleeves and bikini bottom/shorter-length shorts with open-top footwear (barefoot/open sandals) reasonably fit $EBA_{beach/pool}(t)$. The best fit indicates that a majority of beachgoers select the most sun-seeking/highest exposure risk clothing options at hours with peak UV

Table 2 Upper and lower exposed body areas (EBA) based on clothing selection (from Petersen et al. [10])

Upper body		Lower body	
Clothing	EBA_{upper} [%]	Clothing	EBA_{lower} [%]
Bikini top	46.5	Bikini bottom	38.5
Tank top	26.5	Swimming trunks	35.0
Short sleeves	13.4	Short-length shorts or short skirt	28.0
3/4-length sleeves	11.0	Knee-length shorts or skirt	17.5
Long sleeves	8.5	3/4-length trousers or skirt	12.0
		Long trousers or skirt	3.5

Table 3 Percent exposed body area as a function of time, $EBA_{beach/pool}(t)$, and the associated clothing choices (on the upper $f_{upper,beach/pool}(t)$ and lower body $f_{lower,beach/pool}$ expressed in relative percentage) that provided the best fit to the function, $EBA\_fit_{beach/pool}(t)$, for a female body model in beach/pool setting

Time	$EBA_{beach/pool}(t)$ [%]	$f_{upper,beach/pool}(t)$ [1]			$f_{lower,beach/pool}(t)$ [1]		$EBA\_fit_{beach/pool}(t)$ [%]
		Bikini	Tank top	Short sleeves	Bikini	Shorts (short length)	
08:00	49.1	0.00	0.00	1.00	0.73	0.27	49.2
09:00	58.6	0.10	0.40	0.50	0.85	0.15	58.9
10:00	66.1	0.23	0.50	0.27	1.00	0.00	66.1
11:00	71.6	0.33	0.67	0.00	1.00	0.00	71.6
12:00	75.2	0.51	0.49	0.00	1.00	0.00	75.2
13:00	76.8	0.59	0.41	0.00	1.00	0.00	76.8
14:00	76.5	0.57	0.43	0.00	1.00	0.00	76.4
15:00	74.2	0.46	0.54	0.00	1.00	0.00	74.2
16:00	69.9	0.25	0.75	0.00	1.00	0.00	70.0
17:00	63.7	0.20	0.40	0.40	1.00	0.00	63.8
18:00	55.5	0.00	0.40	0.60	0.85	0.15	55.6

intensity (i.e., at $t = 12{:}00$–14:00, over 50% of beachgoers would select both a bikini top and bottom).

2.4.2 Clothing choices in other outdoor settings

Public outdoor settings away from the beach or pool are associated with the lowest EBA's and most conservative beach vacation clothing choices. For other outdoor (OO) sun exposure settings away from the beach/pool, such as in a city/town or parks surrounding the beach, the associated EBA, $EBA_{OO}(t)$, reaches a maximum of 41.3%. This EBA value roughly corresponds to a woman wearing a short-sleeved shirt and a short skirt or shorts (EBA = 41.4%), or a woman wearing a tank top and knee-length skirt or shorts (EBA = 44%). The minimum value of $EBA_{OO}(t)$, 26.4%, reflects common choices of wearing short sleeves and a 3/4-length trousers or skirt (EBA = 25.4%). Following the fitting methodology outlined previously, a simplified selection of women's clothing options of tank top or short sleeves and short-or-3/4-length shorts/trousers/skirt reasonably models $EBA_{OO}(t)$ throughout the day. Details of the calculated clothing choices that provided a best fit to $EBA_{OO}(t)$ are shown in Table 4**.**

2.4.3 Clothing choices in the balcony setting

Given the relative privacy of the balcony setting, EBA's are best modelled by a wider selection of clothing choices than in the beach/pool or other outdoor public settings. The minimum value of $EBA_{balcony}(t)$, 34% ($t = 08{:}00$), is similar to the EBA value from a clothing choice of short sleeves and a knee-length skirt or shorts (EBA = 30.9%). $EBA_{balcony}(t)$ reaches a maximum value of 53% at noon, which corresponds to clothing choices of a tank top and shorter shorts/skirt (EBA = 54.5%) or a short sleeve shirt and bikini bottoms/swim trunks (EBA = 51.9%). Time-resolved distributions of garment combinations that deliver the best fit against $EBA_{balcony}(t)$ are listed in Table 5.

2.5 Activity and body postures within different sun-exposure environments

2.5.1 Activities and postures at the beach/pool

Activity and postures are more highly variable at the beach/pool than in other outdoor exposure settings and require insights from multiple observational studies to define sufficiently. Siani et al. [37] observed that people on the beach, while not in the water, spend 10% of their time in the shade (e.g., under an umbrella), and 90% of their time exposed to direct sunlight. When exposed to direct sunlight out of the water, people spent 35% of the time standing, 45% lying down, and 20% sitting. It was assumed in this model that people spend equal time in the supine and prone positions while lying down and equal time in the reclined and upright positions while sitting. The shading capability of umbrellas was estimated by Grifoni et al. [38] to reduce incoming incident UV irradiance by 5% for a horizontally oriented surface and 20% for a vertically oriented surface. O'Riodan et al. [39] found that on average people spend 14% of their total time at the beach in the water. For this model, it was assumed that this time in the water is a subset of the time in direct sunlight (i.e. 10% shade, 76% direct sunlight on land, 14% direct sunlight in water). For time spent in the water, it is assumed that people are submerged at least up to the hip. As more detailed posture data for water activities are not available in observational studies, this model assumed an unweighted frequency distribution of postures of 33.3% standing, 33.3% breaststroke, and 33.3% backstroke. Clothing choice on land was assumed to follow Table 3 regardless of whether the time was spent in the sun or the shade. For the portion of time spent in the water, it is assumed that only

Table 4 Exposed body area as a function of time, EBA_{OO}(t), and the associated clothing choices (on the upper $f_{upper,OO}$(t) and lower body $f_{lower,OO}$ expressed in relative percentage) that provided the best fit to the function, EBA_fit_{OO}, for a female body model in outdoor settings away from the beach and pool

Time	$EBA_{OO}(t)$ [%]	$f_{upper,OO}(t)$ [1]		$f_{lower,OO}(t)$ [1]		$EBA\_fit_{OO}(t)$ [%]
		Tank top	Short sleeves	3/4 length	Short length	
08:00	26.4	0.00	1.00	0.95	0.05	26.3
09:00	31.5	0.05	0.95	0.70	0.30	31.0
10:00	35.5	0.10	0.90	0.50	0.50	34.8
11:00	38.5	0.15	0.85	0.30	0.70	38.7
12:00	40.4	0.15	0.85	0.20	0.80	40.3
13:00	41.3	0.20	0.80	0.15	0.85	41.7
14:00	41.1	0.20	0.80	0.15	0.85	41.7
15:00	39.8	0.15	0.85	0.25	0.75	39.5
16:00	37.6	0.10	0.90	0.30	0.70	38.0
17:00	34.2	0.10	0.90	0.50	0.50	34.8
18:00	29.8	0.05	0.95	0.80	0.20	29.4

Table 5 Exposed body area as a function of time, EBA $_{balcony}(t)$, and the associated clothing choices (on the upper $f_{upper,balcony}(t)$ and lower body $f_{lower,balcony}$ expressed in relative percentage) that provided the best fit to the function, EBA_fit $_{balcony}(t)$, for a female body model in the balcony setting

Time t	$EBA_{balcony}(t)$ [%]	$f_{upper,balcony}(t)$ [1]				$f_{lower,balcony}(t)$ [1]				$EBA\_fit_{balcony}(t)$ [%]
		Bikini	Tank top	Short sleeves	3/4 sleeves	Bikini	Short length	Knee length	3/4 length	
08:00	33.7	0.00	0.30	0.50	0.20	0.00	0.30	0.50	0.20	34.3
09:00	40.2	0.00	0.40	0.60	0.00	0.00	0.40	0.50	0.10	39.9
10:00	45.4	0.05	0.55	0.40	0.00	0.05	0.45	0.50	0.00	45.6
11:00	49.2	0.15	0.45	0.40	0.00	0.10	0.50	0.40	0.00	49.2
12:00	51.6	0.15	0.55	0.30	0.00	0.15	0.55	0.30	0.00	52.0
13:00	52.7	0.20	0.50	0.30	0.00	0.15	0.55	0.30	0.00	53.0
14:00	52.5	0.20	0.50	0.30	0.00	0.15	0.55	0.30	0.00	53.0
15:00	50.9	0.10	0.60	0.30	0.00	0.10	0.60	0.30	0.00	50.5
16:00	48.0	0.10	0.50	0.40	0.00	0.05	0.55	0.40	0.00	47.6
17:00	43.7	0.05	0.45	0.50	0.00	0.00	0.50	0.50	0.00	43.8
18:00	38.1	0.00	0.35	0.65	0.10	0.00	0.30	0.60	0.10	38.2

swimming clothes (i.e. bikini top and bottom) are worn. Postures extrapolated from these observations and assumptions across each of the beach/pool sun exposure conditions are presented in Table 6.

2.5.2 Activities and postures in other outdoor settings

Activities and postures used to represent typical activities at other outdoor settings away from the beach or pool are drawn from Schmalwieser et al. [17], who concluded that walking, cycling, sightseeing and sitting in a sidewalk café each resulted in similar levels of UV exposure. Only the activity of shopping was observed to significantly reduce UV exposure by about 75%, as people move between indoor shops and outdoor settings. As there are no time-resolved studies available, an unweighted activity distribution of 33.3% walking, 33.3% sitting in a sidewalk café and 33% shopping was assumed in this model, with corresponding postures and surrounding solar radiation assigned as standing with 70% ambient radiation, sitting upright with 70% ambient radiation, and standing with 30% ambient radiation, respectively. Body surface orientation to the sun was randomly distributed in this model, as sun exposure in this setting is largely incidental and not pursued as part of sun-seeking or intentional sun exposure behavior.

2.5.3 Activities and postures in the balcony setting

As balconies are generally smaller spaces without room for engaging in varied physical activity, sitting upright was assumed as the predominant posture in the balcony environment.

Table 6 Representative percentages of time spent engaging in various sun-exposure conditions and body postures while at the beach/pool

Location and sun-exposure condition (percentage of overall time spent in location/sun-exposure condition)	Posture (percentage of time in respective location/sun-exposure condition spent in posture)
Direct sunlight in water (14%)	Standing (33.3%)
	Breaststroke (33.3%)
	Backstroke (33.3%)
Shade on land (10%)	Sitting (upright) (100%)
Direct sunlight on land (76%)	Standing (35%)
	Sitting (upright) (10%)
	Sitting (reclining) (10%)
	Lying down (supine) (22.5%)
	Lying down (prone) (22.5%)

3 Results

Erythemally effective irradiance to all body sites was calculated from sunrise to sunset for the described representative postures, clothing choices, and sun exposure settings (i.e. beach/pool, city/town or other outdoor environments, and shaded balcony) common to a beach vacation. These calculations were used to determine acute body site-specific UV exposure across a range of behaviors and cumulative UV exposures during a representative week at a beach vacation setting.

3.1 Time- and posture-dependent irradiance in a high sun exposure scenario

At mid-day in the beach setting, the body model with highest EBA clothing choice (bikini) experiences high erythemal irradiance at multiple body sites across all activities and postures. Acute irradiances at noon ($t = 12$:00, solar elevation $\alpha = 76°$) during common beach postures and activities are listed for different body sites in Table 7 and illustrated in Fig. 3, for activities that include walking on the beach (Fig. 3a), standing in waist-deep water (Fig. 3b), laying on the beach (Fig. 3c), and sitting under an umbrella (Fig. 3d). In the lying down posture, shielded parts of the body do not receive any UV exposure, while horizontally oriented body parts facing the sun receive the highest acute irradiance of any body part in any position (9.8 SED/h). When in the standing upright posture, the nose and ear regions of the head as well as the chest and shoulders receive similar maximum UV exposure (9.8 SED/h), whether standing on land (Fig. 3a) or in waist-deep water (Fig. 3b). Exposure can be highly variable within a body site, with individual facial polygons on the cheek on a standing figure at noon receiving UV exposures as high as 9.1 SED/h close to the nose down to 5.5 SED/h on the side of the face. Even when largely shaded by structures like an umbrella that reduce direct solar irradiance, diffuse irradiance from the unobscured sky and surrounding surfaces still resulted in significant UV exposure. This is illustrated in Fig. 4d, where the chest, stomach and feet of a person lying under a shaded umbrella at noon were subject to erythemally effective irradiances greater than 5 SED/h.

Time-resolved irradiance and radiant exposure data for a full day at the beach in a bikini highlights the times of day and body sites of greatest concern to erythemal overexposure, irrespective of activity or posture. Table 8 describes the erythemal exposure experienced over body sites during a distribution of typical beach/pool behaviors throughout the course of a typical day for the highest EBA clothing choice. These data clearly show the evolution of erythemal solar irradiance over the day, with highest values observed at mid-day hours of high solar elevation, particularly $t = 11$:00–14:00. All body sites experience cumulative radiant exposures greater than 35 SED, with greatest erythemal exposures (~ 50 SED) observed at body sites known to be highly susceptible to sunburn (e.g. head, shoulders and chest). From more typical daily time spent at the beach or pool (1.1 h spent from $t = 7$:00–12:00, 1.6 h spent from 12:00 to 15:00, and 0.8 h spent from 15:00 to 19:00), all body sites still experience over 13 SED of total erythemal exposure.

Table 7 Maximum erythemally effective irradiance at $t = 12$:00 on different body sites on a female body model with maximal exposed body area clothing options (i.e. bikini)

Body part	Standing		Lying down (prone)		Lying down (supine)		Sitting (upright)		Sitting (reclining)	
	UV index	SED/h	UV index	SED/h	UV index	SED/h	UV index	SED/h	UV index	SED/h
Hip	6.7	6.1	10.8	9.7	10.9	9.8	8.9	8.0	10.8	9.7
Abdomen	5.5	5.0	10.9	9.8	10.9	9.8	8.9	8.0	10.8	9.7
Chest	10.9	9.8	10.9	9.8	10.9	9.8	10.9	9.8	10.9	9.8
Neck	6.1	5.5	10.9	9.8	10.9	9.8	6.1	5.5	7.9	7.1
Head	10.9	9.8	10.9	9.8	10.9	9.8	10.9	9.8	10.9	9.8
Shoulders	10.9	9.8	10.8	9.7	10.8	9.7	10.9	9.8	10.9	9.8
Upper arm	5.0	4.5	10.9	9.8	10.9	9.8	10.3	9.3	7.9	7.1
Forearm	6.7	6.1	10.9	9.8	10.9	9.8	10.3	9.3	10.9	9.8
Hand	8.9	8.0	10.9	9.8	10.9	9.8	10.9	9.8	10.9	9.8
Thigh	6.1	5.5	10.9	9.8	10.9	9.8	10.9	9.8	10.9	9.8
Shin	8.4	7.5	10.9	9.8	10.9	9.8	10.6	9.5	10.9	9.8
Foot	10.9	9.8	10.9	9.8	10.9	9.8	10.8	9.7	10.9	9.8

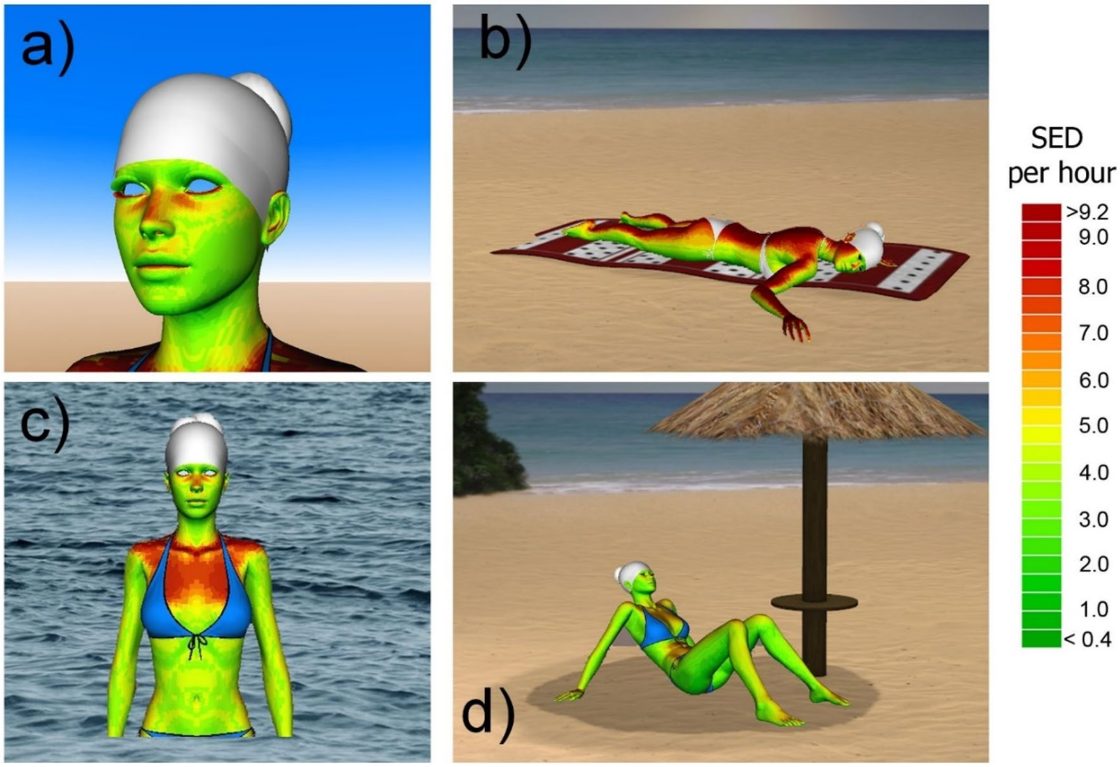

Fig. 3 Examples of the erythemally effective irradiance patterns on the body surfaces of the chosen body model in relevant postures and clothing within the different activities common to beach sun exposure during high solar elevations ($t = 12{:}00$, solar elevation $\alpha = 76°$)

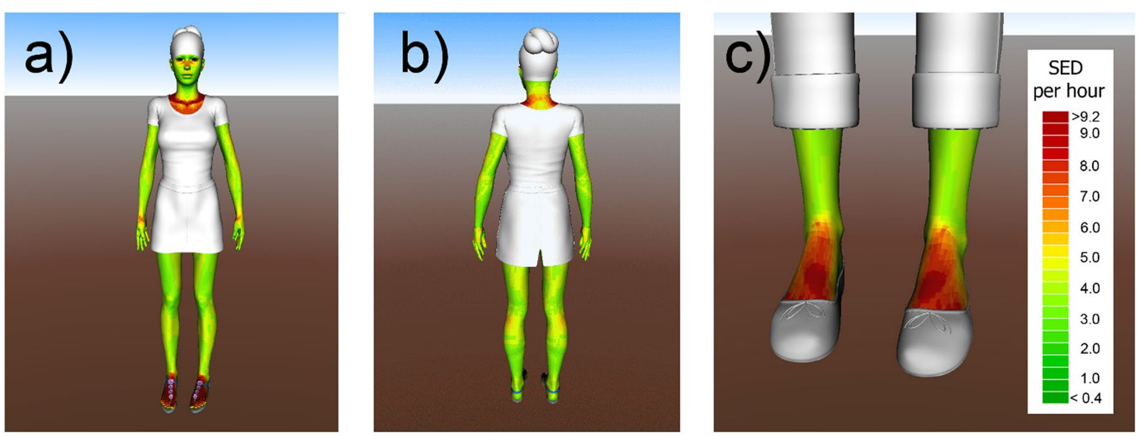

Fig. 4 Erythemally effective irradiance patterns for outdoor locations away from the beach/pool, depicted for the typical garment combination specific for noon: **a** anterior view; **b** posterior view; **c** magnified view of altered exposure pattern on the lower leg and foot based on a more photoprotective garment selection for the legs/feet

3.2 Erythemal exposure in different solar settings with typical clothing selections

Daily erythemally effective radiant exposure at each body site highlights areas of high vulnerability in different settings and clarifies each setting's significant contributions to a full week of beach vacation exposure. Standard erythemal doses calculated for typical behaviors and clothing choices for both a full day and typical daily time spent in each differentiated solar exposure settings are described in Table 9.

Comparison of daily exposures in the beach/pool setting with a single high-EBA clothing choice (Table 8) against mixed clothing choices in the same setting (Table 9) highlights body sites most susceptible to UV dose mitigation

Table 8 Maximum erythemally effective irradiance and cumulative erythemal radiant exposure on different body sites on a female body model while at the beach with maximal EBA clothing options (i.e. bikini), assuming a representative distribution of activities. Erythemal irradiances at $t = 7{:}00$ and $t = 19{:}00$ are < 0.1 SED/h in all settings, and thus do not contribute significantly to total daily exposures and are not listed in this table. Cumulative exposure given for a full day at the beach and typical daily time spend at the beach (3.6 h distributed throughout the day)

Body site	Maximum erythemally effective irradiance, typical postures, bikini only [UV index = 0.9 SED/h]											Cumulative daily erythemal exposure	
	t = 08:00	t = 09:00	t = 10:00	t = 11:00	t = 12:00	t = 13:00	t = 14:00	t = 15:00	t = 16:00	t = 17:00	t = 18:00	Full day of sunlight at beach [SED]	Typical daily beach time (3.6 h total) [SED]
Hip	1.1	2.7	4.6	6.4	7.5	7.5	6.3	4.5	2.6	1.1	0.3	40.1	14.2
Abdomen	1.1	2.7	4.6	6.4	7.4	7.4	6.3	4.5	2.6	1.1	0.3	40.0	14.1
Chest	1.4	3.3	5.9	8.3	9.7	9.7	8.2	5.8	3.2	1.3	0.3	51.4	18.3
Neck	1.2	2.8	4.9	6.7	7.8	7.8	6.6	4.8	2.8	1.2	0.3	42.2	14.9
Head	1.4	3.4	6.0	8.4	9.9	9.9	8.4	5.9	3.3	1.3	0.3	52.4	18.6
Shoulders	1.4	3.4	5.9	8.4	9.9	9.8	8.3	5.9	3.3	1.3	0.3	52.1	18.5
Upper arm	1.1	2.7	4.6	6.3	7.3	7.3	6.2	4.5	2.6	1.1	0.3	39.6	14.0
Forearm	1.2	2.9	5.0	6.9	8.1	8.1	6.8	4.9	2.8	1.2	0.3	43.4	15.3
Hand	1.3	3.0	5.3	7.5	8.8	8.8	7.4	5.3	3.0	1.2	0.3	46.7	16.6
Thigh	1.1	2.6	4.5	6.2	7.2	7.2	6.1	4.4	2.5	1.0	0.3	38.8	13.7
Shin/calf	1.1	2.7	4.8	6.7	7.8	7.8	6.6	4.7	2.6	1.1	0.3	41.6	14.7
Foot	1.2	2.9	5.2	7.3	8.6	8.5	7.2	5.1	2.8	1.2	0.3	45.3	16.1

Table 9 Daily erythemally effective radiant exposure on different body sites on a female body model while at representative beach vacation solar settings, assuming representative postures and clothing choices. Cumulative exposure is given for both a full day spent in each setting, and the typical daily time spend at each setting

Body site	Cumulative erythemal exposure [SED]					
	Beach or pool		Outdoor activities		Shaded balcony	
	Full-day total	Typical daily total (3.6 h)	Full-day total	Typical daily total (2.9 h)	Full-day total	Typical daily total (1.7 h)
Hip	17.4	6.9	0.0	0.0	1.4	0.1
Abdomen	18.0	7.2	0.0	0.0	1.5	0.2
Chest	47.2	17.4	5.0	1.3	7.3	0.8
Neck	42.2	14.9	20.1	5.1	15.5	1.8
Head	52.4	18.6	33.7	8.5	24.1	2.8
Shoulders	48.0	17.6	5.0	1.3	7.3	0.8
Upper arm	39.6	14.0	23.1	5.8	24.1	2.8
Forearm	43.4	15.3	25.7	6.5	24.1	2.8
Hand	46.7	16.6	30.0	7.6	24.1	2.8
Thigh	38.1	13.6	25.5	6.4	6.3	0.6
Shin/calf	41.6	14.7	28.8	7.3	23.2	2.7
Foot	45.3	16.1	33.4	8.5	24.1	2.8

via clothing choice. In these two conditions, the calculated UV exposures at the extremities (head, neck, arms and legs) remained the same, while exposures on body sites on the trunk (shoulders, chest, abdomen, and hip) decreased in the mixed clothing choice condition. The hip and abdomen received markedly less exposure when the female model employed typical clothing choices than with the highest EBA (17–18 SED versus ~ 40 SED in a full day, respectively). The shoulders and chest also experienced a drop in exposure, though not nearly as drastic (47–48 SED versus ~ 52 SED in a full day for mixed and high EBA clothing choices, respectively). These differences can be attributed to the relative coverage provided by clothing options in the beach setting; while all clothing options leave portions of the extremities exposed, only the most conservative top choices fully cover the shoulders and chest, and only the highest EBA clothing choice (bikini) leaves the abdomen and hip exposed.

The impact of clothing choice on erythemal exposure doses was also observed in differences in UV exposure at specific body sites between exposure settings. For example, setting-specific differences in clothing choice are reflected by significant differences in exposure at the hip, abdomen and shoulders between the beach/pool versus other outdoor settings. Specific localized patterns of mid-day irradiance in the city/town setting are visualized in Fig. 4. As in the beach setting, high UV exposures in the city/town/other outdoor settings were observed on the bridge of the nose, chest/decolletage and feet (Fig. 4a), as well as the neck and calves (Fig. 4b). In city/town/other outdoor settings, however, no erythemal irradiance was calculated at the abdomen and hips throughout the day, as this model assumed that these body sites were always covered in this setting. Likewise, erythemal exposure at the shoulders was only 15% of that calculated at the head for a full day in this setting (compared to 92% in the beach/pool setting), as the model calculated that short-sleeved shirts are typically worn at least 80% of the time outdoors away from the beach/pool.

Though each setting is subject to different solar conditions, clothing choices, and activities and postures, each location contributes significantly to cumulative UV exposure totals. For a typical beach vacation day, even though only about 3.6 h (30% of daylight hours) is spent at the beach or pool, much of this is during peak sun hours (12:00–15:00) in high-solar-intensity settings. This setting is thus the greatest contributor to total exposure expected in a full day (~ 40–50%). In contrast, the shaded balcony may be considered a lower risk setting, given that typical time spent on balconies is low (14% of daylight hours) and mostly at times of lower solar intensity (before noon or after 15:00). Figure 5 visualizes UV irradiance patterns and typical clothing choices in the shaded balcony setting in the morning, midday, and early afternoon. Perhaps surprisingly, this setting is still a significant contributor to daily beach vacation solar exposure totals, adding ~ 3 SED per day at higher-exposure body sites.

3.3 Cumulative total UV exposure for a 1-week vacation at a beach destination

Cumulative erythemal radiant exposure totals were calculated to evaluate the relative contribution of 1 week beach vacations to average annual UV exposure totals and lifetime skin health risk. Total erythemal exposure accumulated at each body site during a full week was calculated by summing exposure contributions across weighted distributions representative of time spent in each exposure setting, clothing choice, activity and postures. Cumulative erythemal doses received by each body part over the course of a typical

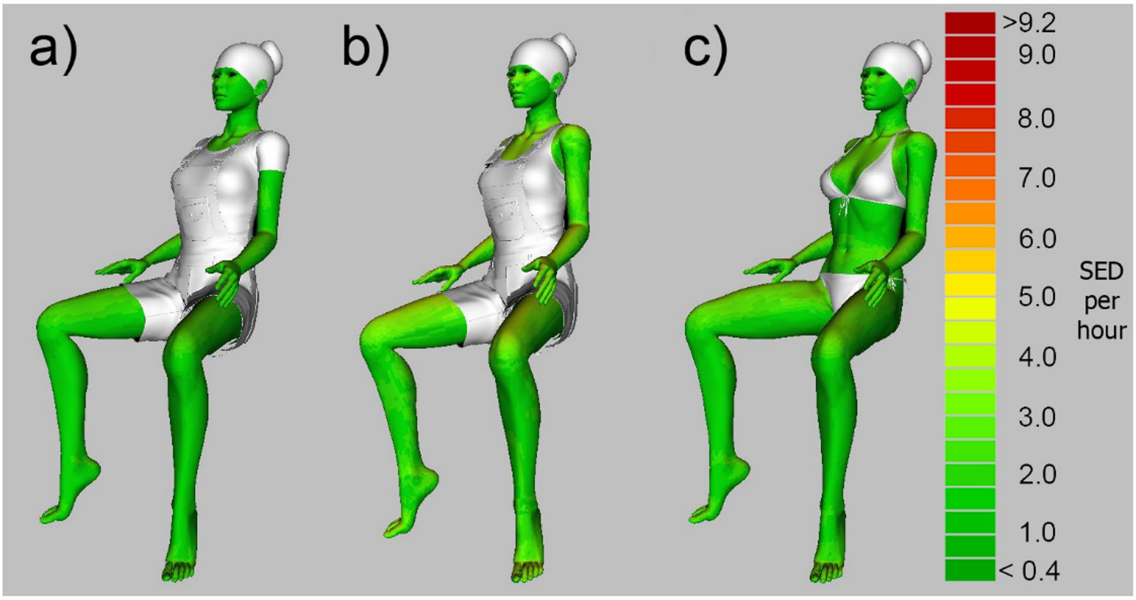

Fig. 5 Erythemally effective UV irradiance patterns while seated on a shaded balcony, depicted for the most typical garment combination for the specific time of day: **a** in the early morning (09:00); **b** in the late morning (11:00); and **c** in the early afternoon (13:00)

vacation day, as well as sums of exposure over a 7-day vacation, are listed in Table 10**.**

Based on this model and selected clothing, activity, and posture conditions, individuals of all skin phototypes experience risk of UV overexposure and erythema through a week-long beach vacation. Cumulative erythemal radiant exposure can be expressed in units of the minimal erythemal dose (MED) for the different skin phototypes according to Fitzpatrick [40], as depicted in Table 10 for typical full week beach vacation exposures: 1 MED is approximated as 100 J/m^2 for Fitzpatrick skin phototype (FSP) I; 200 J/m^2 for FSP II; 400 J/m^2 for FSP III; 650 J/m^2 for FSP IV; 850 J/m^2 for FSP V; and 1200 J/m^2 for FSP VI. An MED exceeding 1 in a single day indicates a risk of expression of erythema (sunburn) for a subject of that skin type. The head experiences the highest level of UV exposure, with exposures that exceed 200 MEDs across a full week beach vacation for an individual with FSP I (light skin, always

Table 10 Daily average and 7-day total cumulative erythemal exposure from a week-long beach vacation per body site, assuming full-day exposure from a typical distribution of time spent at the beach/pool, city/town, and balcony settings wearing typical clothing. 7-day total cumulative exposure displayed in units of representative minimal erythemal doses (MED) for different Fitzpatrick skin phototypes (FSP) I–VI

Body site	Daily average UV exposure [SED]	Typical 7-day UV exposure total (MED per FSP)					
		MED FSP I (100 J/m^2)	MED FSPII (200 J/m^2)	MED FSP III (400 J/m^2)	MED FSPIV (650 J/m^2)	MED FSP V (850 J/m^2)	MED FSP VI (1200 J/m^2)
Hip	7.0	49.0	24.5	12.3	7.5	5.8	4.1
Abdomen	7.4	51.8	25.9	13.0	8.0	6.1	4.3
Chest	19.5	136.5	68.3	34.1	21.0	16.1	11.4
Neck	21.8	152.6	76.3	38.2	23.5	18.0	12.7
Head	29.9	209.3	104.7	52.3	32.2	24.6	17.4
Shoulders	19.7	137.9	69.0	34.5	21.2	16.2	11.5
Upper arm	22.6	158.2	79.1	39.6	24.3	18.6	13.2
Forearm	24.6	172.2	86.1	43.1	26.5	20.3	14.4
Hand	27.0	189.0	94.5	47.3	29.1	22.2	15.8
Thigh	20.6	144.2	72.1	36.1	22.2	17.0	12.0
Shin/calf	24.7	172.9	86.5	43.2	26.6	20.3	14.4
Foot	27.4	191.8	95.9	48.0	29.5	22.6	16.0

burns, does not tan), and 17 MEDs for an individual with FSP VI (dark brown or black skin, always tans). It is not only the head that is vulnerable across skin types; in fact, all body sites (except the hip and abdomen) across all skin types are exposed to UV doses that exceed 7 MED for a weeklong beach vacation, or 1 MED/day. The head, forearm, hands, shin/calf, and foot receive at least double this 7 MED/week (1MED/day) exposure threshold for erythemal risk across all skin types. For individuals with lighter skin tones, the sun exposure levels during a single day may be 10–30 times higher than the MED.

4 Discussion

4.1 Model comparison against real-life beach studies

The modelling described in this work is a generalizable method that can be leveraged to generate insights on UV exposure in diverse global settings. The validity of this approach is confirmed through comparison of calculations from this model with erythemal radiant exposure values from beach studies where solar conditions were directly measured. Petersen et al. [41] measured an average exposure of 9.4 SED/day (over 7.4 h/day of solar exposure) on a wrist-mounted UV dosimeter on people in Tenerife during the first week of March. Compared with the location in which this model was based (Tampa, FL), Tenerife has a lower solar elevation ($\alpha \leq 54°$) and shorter UV exposure duration. Decreasing the solar elevation in the computational model accordingly decreases erythemal exposure by a factor 0.73, and shortening the length of daylight to what is typically observed in Tenerife decreases erythemal exposure by a factor of 0.62. A cloud cover modification factor of 1.0 (indicating clear sky or light cloud cover) was assumed for the model in Tampa in late April/early May; adding an additional correction factor of 0.9–0.85 is more representative of Tenerife in March [28]. Application of these correction factors to this UV exposure model translates a predicted average daily forearm exposure of 24.6 SED/day expected in Tampa, FL in April/May to 10.0–9.5 SED/day expected in Tenerife in March, consistent with the directly observed 9.4 SED/day.

Likewise, Kohli et. al. [42] collected radiometry data for 5 consecutive days from 27 May to 01 June at Upham Beach in St. Petersburg, FL and measured approximately 30.5 SEDs on a horizontal receiver over approximately 3.6 h during two intervals around peak sun intensity, specifically, the hours of $t = 10{:}00$–$12{:}00$ and $t = 13{:}00$–$15{:}00$, corresponding to an average erythemal irradiance of ~ 8.5 SED/h. As this location and time of year are similar, and this study explicitly found minimal impact from cloud cover over a 5 day period, no additional solar/weather correction factors are necessary for comparison between this study and the presented UV exposure model. Irradiances from the presented computational model are consistent with the observed values, with the model yielding maximal body site exposure irradiances at the horizontally oriented areas of the head and shoulders in the beach/pool setting of about 6–10 UV index (~ 5–9 SED/h) at the $t = 11{:}00$, 12:00, 14:00 and 15:00 timepoints (as shown in Table 8).

4.2 Comparison to annual exposure contributions and public health outcomes

Results from this computational model confirm observations that cumulative UV exposures from beach vacations contribute significantly to lifetime totals at specific body sites while adding implementation flexibility and additional detail on exposure patterns across the body. The presented model calculated an accumulation of 172.2 SED at the forearm over a typical 7-day beach vacation in Tampa, FL. This level of exposure nearly matches or exceeds the average total annual routine UV exposure of people living in upper latitudes of the North American continent. For example, UVR dosimeter measurements in Denmark at a latitude of 56°N, (comparable to latitudes in parts of Alaska and Canada), estimate an average annual UV exposure of 173 SED, with dosages varying from 224 SED for outdoor workers (gardeners) to 132 SED for indoor workers [9]. Individuals living at such high latitudes with lower average UV index likely have not developed photoadaptation sufficient to modulate the impacts of the high UV exposure beach environment and may experience exaggerated negative impacts from this sudden influx of UV exposure. These impacts may not be as evident in vacationers from more southern latitudes in North America accustomed to higher annual UV doses, estimated to be 272 SED at 39°N (a latitude shared by San Francisco, Denver and New York) [43], and 280 SED at 34°N (a latitude shared by Los Angeles, Dallas and Atlanta) [44]. The 172.2 SED/week calculated in this model still exceeds 50% of typical annual UV exposure at these southern locations. Modelling efforts tailored to account for such individual differences in annual solar exposure and photoadaptation could provide personalized insights on the risks associated with large UV doses.

One potential consequence of the large cumulative UV exposures calculated for beach vacations is a quantifiable increased risk for the development of skin cancer. Risk of developing non-melanoma skin cancer (NMSC) at a specific body site, (R), has been shown in multiple studies to increase as a power function of UV exposure, (D), [45–47], i.e. $\ln(R) = A_b \, ln\ (D)$, where A_b is a biological amplification factor. For a light skinned population (FSP I–III), $A_b \sim 2$ [43], with specific values varying from ~ 1–3 for different types of skin cancer, different parts of the body, and male & female populations [44]. A 50–100% increase of annual UV exposure attributable to an additional single week-long Florida beach vacation for a typical North American resident may thus increase NMSC risk by a factor of 2–4 (assuming $A_b \sim 2$) for body sites with relatively high typical exposure. Sites on the trunk that are more covered during the year may see a relative increase in annual UV exposure from a beach vacation significantly greater than 50–100%. Additionally, A_b (and thus NMSC risk) is higher at these body sites in some populations; Moan et al. [47] describes A_b for squamous cell carcinoma as higher for males on the trunk and neck (3.13) than on the head (2.34). These comparisons clearly indicate the critical role of engaging in proper sun protection and sun-safe behavior during beach vacations toward reduction of NMSC risk and positive impacts on overall public health.

4.3 Recommendations for sun protection at the beach

Much of the body-site-specific UV overexposure risk highlighted in this model may be mitigated through sun protective attire/style and shade-seeking. Though seeking shade is recommended to and pursued by skin-safe beach goers to reduce UV exposure from direct sunlight, it does not provide full protection. Results from this computational model indicate that during a full day spent in a shaded balcony setting, frequently exposed body sites like the head, upper arms, forearms, hands and shins received as much as 24.1 SED, indicating a significant risk for UV overexposure for most skin types. There are some attire/style options that can provide additional protection to these extremities. Head coverings [48] and certain hairstyles [49] as well as beards [50] can significantly help to reduce some associated UV exposure on the head, though they may still leave areas of the face vulnerable to high UV exposure from diffuse solar irradiance. Closed shoes may bring UV exposure of the feet down to zero, but they are not often worn in the recreational beach setting. Similarly, clothing choices that cover the neck, shoulders, forearm and shins are not frequently observed in high-temperature beach vacation settings.

Topical sun protection products can provide UV protection to body sites that may be difficult or inconvenient to cover with clothing during a beach vacation. UV exposure calculations from the presented model can be combined with erythemal exposure thresholds for different skin phototypes to help inform recommendations for topical sun protection. For example, the presented model calculates highest UV exposure from a full day spent exclusively at the beach to be 52.4 SED on the head. This corresponds to a dose about 52 times greater than the MED for individuals with FSP I, 26 times greater than the MED for individuals with FSP II, and 4 times greater than the MED for individuals with FSP IV. Based on these values, compliant application of topical sunscreens with sun protection factors (SPF's) of at least 50, 30 and 5 might be recommended to these populations, respectively, to bring their daily erythemal exposure doses below 1 MED and minimize their risk of sunburn.

Repeated daily exposure to solar irradiation can damage the skin and necessitate higher SPF recommendations based on an individual's increased susceptibility to sunburns. Specifically, repeated sub-erythemal exposure has been shown in some cases to reduce personal MED by up to 30% [51]. Though UV exposure has been shown to be protective in some cases, this is only after sufficient recovery time. In one study [52], the recovery period for the skin from erythema response was 24 to 48 h, after which a slight protective effect from UV exposure only appeared after a 4-day waiting period. Similarly, Kollias et al. [53] observed enhanced erythema, pigmentation and desquamation with repeated MED-level UV exposure within 24 h, with photoprotective effects of repeated UV exposure evident only after 2 or more days. Given that daily erythemal exposure is common in this setting, individuals on beach vacations are likely to experience the photosensitization of repeated exposure to erythemal radiation without the benefit of photoprotection offered by sufficient recovery time.

Various additional behavioral, biological, and environmental factors in the beach vacation setting drive the need for sun protection recommendations beyond the hypothetical minimum needed to reduce an individual's personal exposure below 1 MED per day. For example, saltwater exposure may enhance skin sensitivity for erythema by as much as 20–30% [54, 55]. Additionally, sweating caused by heat or physical activity may additionally decrease MED by approximately 15% [56]. Together with the aforementioned impacts from repeated daily erythemal UV exposure, these factors may result in a combined personal MED reduction of > 50%. Higher SPF levels would be needed to compensate not only for this suppression of MED, but also for application of less than the recommended density of topical sunscreens (2 mg/cm^2). Given such behavioral and biological complexities in the beach setting, this model may serve better as a guide to encourage overall safer sun protective behaviors across populations of all skin types than a tool to recommend "sufficient" minimal sun protection for individuals.

4.4 Considerations to interpretation of UV over-exposure risk

The presented modelling provides a more complete picture of whole-body sun exposure in the beach setting than previous work by utilizing behavioral information simplified sufficiently for incorporation into the described framework. The presented female body model represents a typical individual experiencing UV overexposure in the beach vacation setting. Though typical women's clothing choices were selected for this model, it should be considered that the data from Peterson et al. [10] from which clothing choices are drawn comes from the daily diaries of men *and* women ($N = 11$ and $N = 14$, respectively) in Tenerife. Additionally, it should be noted that female clothing choices in Tenerife may be more conservative than in the warmer and sunnier Tampa. Likewise, participants of this observational study originated from Copenhagen (Denmark, 55°N) and may not share typical behaviors and cultural attitudes with the typical North American vacationers in Tampa, FL. Further, clothing was assumed to be completely protective; this simplifies calculations and provides a powerful visual delineation of the impact of clothing styles on UV exposure patterns on the body. However, it should be noted that the level of UV protection provided by clothing, although generally high, depends upon numerous factors such as material, weave, age, etc.

This approach to estimating solar exposure is uniquely flexible in that it can incorporate real-life behavioral information and consequently inform UV over-exposure risk among specific sub-populations. Calculations in this work incorporate typical behavior and clothing for beachgoers as described in Peterson et al. [10]. Behavior of an atypical "sun seeker", who comes to the beach for a single day and spends much of the time in the high sun exposure environment, may require additional considerations to appropriately model UV exposure. For example, a "sun seeking" individual may choose to spend more time in the beach/pool setting explicitly tanning in a supine, prone or reclining position in direct sunlight. There exists an opportunity to more precisely evaluate sun over-exposure among high-risk individuals by directly incorporating behavioral data from explicitly "sun-seeking" beach vacationers into the presented model.

Modelling itself is useful for capturing and visualizing the incident flux of erythemal UV radiation on skin surfaces, but evaluation of consequent skin health risks requires consideration of inherent vulnerabilities of individuals to solar exposure. This is touched upon in this work through evaluations of sunburn risk based on typical MED's for different Fitzpatrick skin types. This analysis, however, does not capture the tendency for subjects with intermediate skin types to tan and develop unevenly distributed photoadaptation on frequently exposed body parts through the warmer spring and summer months. Though this type of photoadaptation may reduce incidence of erythema from sun over-exposure, the connection to other cumulative skin health risks may still be significant. Additionally, susceptibility to adverse health skin effects from UV exposure can be increased by certain sensitizing topical or systemic medications and genetic predisposition.

4.5 Novelty and future directions

3D body modelling has great utility as a tool in the field of quantitative UVR-related human health [57, 58], and, when used in conjunction with radiative transfer models (e.g. [20, 21, 25, 59]), enables the quantification of previously unknown information pertaining to body-site UV exposure across a wide set of contexts incorporating diverse behavioral variables. Detailed mapping of UV irradiance on the human body allows compelling visualization of sunburn risk reflective of the sunburn patterns familiar to any beachgoer who has spent too much time in the sun. These models provide detail and versatility to sun exposure risk projections which enables critical analysis of photoprotection behaviors (including pursuit of sun-safe activities and settings, clothing choice, and, potentially, use of topical sunscreens). Evaluation of the impact of behavior change in modulating health risks over extended time periods may provide insights relevant to mitigating exposure-related disease states with extended latency periods, such as skin cancer. In the future, this work may be extended to model solar exposure and sunburn risk in settings and activities beyond a typical beach vacation. Further, evaluations of the impact of various components of the solar spectrum (ultraviolet A, visible, infrared radiation), light sources (solar, artificial, industrial) and different action spectra on the skin health of specific body sites may be facilitated by this type of modeling approach.

5 Conclusions

This work demonstrates that week-long beach vacations, while comprising only a small fraction of how a person spends their time annually, can contribute very significantly to a person's cumulative annual UV exposure. 3D-body models bring a unique power to computational UV exposure calculations through visualization of beach vacation activities with detailed mappings of consequent body surface exposure to UV radiation. Resulting calculations on cumulative and acute UV exposure in a variety of settings, postures, and clothing choices demonstrate the versatility of this approach, and its ability to provide both specific and general evaluations of UV exposure risk. The in-silico model of typical cumulative exposures uniquely supports existing estimates of the high UV overexposure risks from beach vacations and the known need for photoprotective measures in this setting through quantitative computational observations. It is well established that UV radiation is a complete carcinogen and that excessive and chronic exposure can have detrimental effects on skin and by extension overall health. This work brings to light body sites that are particularly vulnerable to excessive UV exposure during various beach vacation activities, and the role behaviors such as clothing choice can have in mitigating exposure. These vulnerabilities are highlighted in both educational visual illustrations accessible to a broad audience, as well as numerical calculations allowing for detailed insights of the quantitative relationship between body-site-specific UV exposure and long term skin health risks such as skin cancer Such exposure estimates can better communicate the UV exposure risk associated with beach vacations to a broad population ranging from professional dermatologists to casual beachgoers.

Funding Open access funding provided by University of Veterinary Medicine Vienna. This work was supported by funding from Johnson and Johnson Consumer, Inc.

Declarations

Conflict of interest The authors declare that they have no known competing financial interests or personal relationships that could have appeared to influence the work reported in this paper.

References

1. United States Lifesaving Association. (2019) National lifesaving statistics, 2021, http://arc.usla.org/Statistics/current.asp. Accessed May 2021.
2. EPA, Sun safety monthly average UV index. (2021) https://www.epa.gov/sunsafety/sun-safety-monthly-average-uv-index. Accessed May 2021.
3. Chen, C.-C., & Petrick, J. F. (2013). Health and wellness benefits of travel experiences – a literature review. *Journal of Travel Research, 52*, 709–719.
4. Calzavara-Pinton, P., Sala, R., Arisi, M. C., Bussoletti, C., & Celleno, L. (2013). Photobiology, photodermatology and sunscreens: a comprehensive overview. Part 1: damage from acute and chronic solar exposure. *Giornale Italiano di Dermatologia e Venereologia: Organo Ufficiale, Societa Italiana di Dermatologia e Sifilografia, 148*, 89–106.
5. Office of the Surgeon General. (2014) The surgeon general's call to action to prevent skin cancer, U.S. Department of Health and Human Services, Bethesda, MD, https://www.hhs.gov/sites/default/files/call-to-action-prevent-skin-cancer.pdf. Accessed December 2021.
6. Dobbinson, S., Wakefield, M., Hill, D., Girgis, A., Aitken, J. F., Beckmann, K., Reeder, A. I., Herd, N., Fairthorne, A., & Bowles, K.-A. (2008). Prevalence and determinants of Australian adolescents' and adults' weekend sun protection and sunburn, summer 2003–2004. *Journal of the American Academy of Dermatology, 59*, 602–614.
7. Petersen, B., Wulf, H. C., Triguero-Mas, M., Philipsen, P. A., Thieden, E., Olsen, P., Heydenreich, J., Dadvand, P., Basagaña, X., Liljendahl, T. S., Harrison, G. I., Segerbäck, D., Schmalwieser, A. W., Young, A. R., & Nieuwenhuijsen, M. J. (2014). Sun and ski holidays improve vitamin D status, but are associated with high levels of DNA damage. *The Journal of Investigative Dermatology, 134*, 2806–2813.
8. Schauberger, G., Keck, G., & Cabaj, A. (1992). Trend analysis of solar ultraviolet exposure of the Austrian population caused by holiday patterns since 1969. *Photodermatology Photoimmunology and Photomedicine, 9*(2), 72–77.
9. Thieden, E., Philipsen, P. A., Heydenreich, J., & Wulf, H. C. (2004). UV radiation exposure related to age, sex, occupation, and sun behavior based on time-stamped personal dosimeter readings. *Archives of Dermatology, 140*, 197–203.
10. Petersen, B., Thieden, E., Philipsen, P. A., Heydenreich, J., Wulf, H. C., & Young, A. R. (2013). Determinants of personal ultraviolet-radiation exposure doses on a sun holiday. *British Journal of Dermatology, 168*, 1073–1079.
11. Godar, D. E., Wengraitis, S. P., Shreffler, J., & Sliney, D. H. (2001). UV doses of Americans. *Photochemistry and Photobiology, 73*, 621–629.
12. DeFlorio-Barker, S., Holman, D., Landolfi, R., Arnold, B. F., & Colford, J. M. (2020). Incidence and public health burden of sunburn among beachgoers in the United States. *Preventive Medicine, 134*, 106047.
13. Fernandez-Quiroz, E. L., Gonzales-Chachapoyas, L., Alcantara-Diaz, A. L., Bulnes-Villalta, B., Ayala-Porras, Z., & Toro-Huamanchumo, C. J. (2021). Sunburns among beachgoers in the northern coast of Peru: frequency and factors associated. *PeerJ, 9*, e11473.
14. Holman, D. M., Ragan, K. R., Julian, A. K., & Perna, F. M. (2021). The context of sunburn among US adults: common activities and sun protection behaviors. *American Journal of Preventive Medicine, 60*, e213–e220.
15. Holman, C. D. J., Gibson, I. M., Stephenson, M., & Armstrong, B. K. (1983). Ultraviolet irradiation of human body sites in relation to occupation and outdoor activity: field studies using personal UVR dosimeters. *Clinical and Experimental Dermatology, 8*, 269–277.
16. Diffey, B. L., Larko, O., & Swanbeck, G. (1982). UV-B doses received during different outdoor activities and UV-B treatment of psoriasis. *British Journal of Dermatology, 106*, 33–41.
17. Schmalwieser, A. W., Enzi, C., Wallisch, S., Holawe, F., Maier, B., & Weihs, P. (2010). UV exposure during typical lifestyle. *Photochemistry and Photobiology, 86*, 711715.
18. Schmalwieser, A. W., & Siani, A. M. (2018). Review of nonoccupational personal solar UV exposure measurements. *Photochemistry and Photobiology, 94*, 900–915.
19. Höppe, P., Oppenrieder, A., Erianto, C., Koepke, P., Reuder, J., Seefeldner, M., & Nowak, D. (2004). Visualization of UV exposure of the human body based on data from a scanning UV-measuring system. *International Journal of Biometeorology, 49*, 18–25.
20. Streicher, J. J., Culverhouse, W. C., Jr., Dulberg, M. S., & Fornaro, R. J. (2004). Modeling the anatomical distribution of sunlight. *Photochemistry and Photobiology, 79*, 40–47.
21. Schmalwieser, A. W., Schauberger, G., Grant, W. B., Mackin, S. J., Pope, S. (2006) A first approach in measuring, modeling, and forecasting the vitamin D effective UV radiation. Proceedings of SPIE 6362, Remote Sensing of Clouds and the Atmosphere XI, 63622C (12 October 2006). https://doi.org/10.1117/12.689735
22. Schmalwieser, A. W. (2020). Possibilities to estimate the personal UV radiation exposure from ambient UV radiation

measurements. *Photochemical and Photobiological Sciences, 19*, 1249–1261.

23. Gueymard, C. (1995) SMARTS2, A Simple Model of the Atmospheric Radiative Transfer of Sunshine: Algorithms and Performance Assessment. Professional Paper FSEC-PF-270–95. Florida Solar Energy Center, Cocoa, FL, USA, 1995. http://www.fsec.ucf.edu/en/publications/pdf/FSEC-PF-270-95.pdf. Accessed December 2021.
24. Gueymard, C. A. (2004). The sun's total and spectral irradiance for solar energy applications and solar radiation models. *Solar Energy, 76*, 423–453.
25. Seckmeyer, G., Schrempf, M., Wieczorek, A., Riechelmann, S., Graw, K., Seckmeyer, S., & Zankl, M. (2013). A novel method to calculate solar UV exposure relevant to vitamin D production in humans. *Photochemistry and Photobiology, 89*, 974–983.
26. Weather Spark, https://weatherspark.com/y/16799/Average-Weather-in-Tampa-Florida-United-States-Year-Round. Accessed December 2021.
27. Weather Atlas, https://www.weather-us.com/en/florida-usa/tampa-weather-april#climate_text_1. Accessed December 2021.
28. Foyo-Moreno, I., Alados, I., Olmo, F. J., Vida, J., & Alados-Arboledas, L. S. (2001). On the use of a cloud modification factor for solar UV (290–385 nm) spectral range. *Theoretical and Applied Climatology, 68*, 41–50.
29. CIE (Commission Internationale de l'Eclairage). (1998) Erythema reference action spectrum and standard erythema dose. CIE S007E-1998, CIE Central Bureau, Vienna, Austria.
30. Vanicek, K., Frei, T., Litynska, Z., & Schmalwieser, A. (2000). *UV-Index for the public*. Brussels, Belgium: Publication of the European Communities.
31. Schmalwieser, A. W., Schauberger, G., Januch, M., Nunez, M., Koskela, T., Berger, D., Karamanian, G., Prosek, P., & Laska, K. (2002). Global validation of a forecast model for irradiance of the solar, erythemally effective UV radiation. *J. Optical Engineering, 40*, 3040–3050.
32. Schmalwieser, A. W., Gröbner, J., Blumthaler, M., Klotz, B., De Backer, H., Bolsée, D., Werner, R., Tomsic, D., Metelka, L., Eriksen, P., Jepsen, N., Aun, M., Heikkilä, A., Duprat, T., Sandmann, H., et al. (2017). UV index monitoring in Europe. *Photochemical & Photobiological Sciences, 16*, 1349–1370.
33. WHO (World Health Organization). (2002) Global solar UV index: A practical guide. A joint recommendation of the World Health Organization, World Meteorological Organization, United Nations Environment Programme, and the International Commission on Non-Ionizing Radiation Protection, Geneva, Switzerland.
34. Ou-Yang, H., & Shyr, T. (2017). Sun protection by umbrellas and walls. *Photochemical and Photobiological Sciences, 16*, 1537–1545.
35. Schrempf, M., Thuns, N., Lange, K., & Seckmeyer, G. (2017). Impact of orientation on the vitamin D weighted exposure of a human in an urban environment. *International Journal of Environmental Research and Public Health, 14*, 920.
36. Briceno, L., Harrison, S. L., Heal, C., Kimlin, M., & Paul, G. (2020). Parametric human modelling to determine body surface area covered by sun-protective clothing. *Ergonomics, 63*, 293–306.
37. Siani, A. M., Casale, G. R., Sisto, R., Borra, M., Kimlin, M. G., Lang, C. A., & Colosimo, A. (2009). Short-term UV exposure of sunbathers at a Mediterranean Sea site. *Photochemistry and Photobiology, 85*, 171–177.
38. Grifoni, D., Carreras, G., Sabatini, F., & Zipoli, G. (2005). UV hazard on a summer's day under Mediterranean conditions, and the protective role of a beach umbrella. *International Journal of Biometeorology, 50*, 75–82.
39. O'Riordan, D. L., Steffen, A. D., Lunde, K. B., & Gies, P. (2008). A day at the beach while on tropical vacation – sun protection practices in a high-risk setting for UV radiation exposure. *Archives of Dermatology, 144*, 1449–1455.
40. Fitzpatrick, T. B. (1988). The validity and practicality of sun reactive skin types I through VI. *Archives of Dermatology, 124*, 869–871.
41. Petersen, B., Triguero-Mas, M., Maier, B., Thieden, E., Philipsen, P. A., Heydenreich, J., Dadvand, P., Maier, H., Grage, M.M.-L., Harrison, G. I., Schmalwieser, A. W., Nieuwenhuijsen, M. J., Young, A. R., & Wulf, H. C. (2015). Sun behaviour and personal UVR exposure among Europeans on short term holidays. *Journal of Photochemistry and Photobiology B: Biology, 151*, 264–269.
42. Kohli, I., Nicholson, C. L., Williams, J. D., Lyons, A. B., Seo, I., Maitra, P., Tian, X., Atillasoy, E., Lim, H. W., & Hamzavi, I. H. (2020). Greater efficacy of SPF 100+ sunscreen compared with SPF 50+ in sunburn prevention during 5 consecutive days of sunlight exposure: a randomized, double-blind clinical trial. *Journal of the American Academy of Dermatology, 82*, 869–877.
43. Gurrea, G., & Canada, J. (2007). Study of UV radiation dose received by the Spanish population. *Photochemistry and Photobiology, 83*, 1364–1370.
44. Godar, D. E. (2005). UV doses worldwide. *Photochemistry and Photobiology, 81*, 736–749.
45. Slaper, H., Schothorst, A. A., & Van Der Leun, J. C. (1986). Risk evaluation of UVB therapy for psoriasis: comparison of calculated risk for UVB therapy and observed risk in PUVA-treated patients. *Photodermatology, 3*, 271–283.
46. Diffey, B. L. (1987). Analysis of the risk of skin cancer from sunlight and solaria in subjects living in northern Europe. *Photodermatology, 4*, 118–126.
47. Moan, J., Grigalavicius, M. M., Baturaite, Z., Dahlback, A., & Juzeniene, A. (2015). The relationship between UV exposure and incidence of skin cancer. *Photodermatology, Photoimmunology and Photomedicine, 31*, 26–35.
48. Backes, C., Religi, A., Moccozet, L., Vuilleumier, L., Vernez, D., & Bulliard, J. L. (2018). Facial exposure to ultraviolet radiation: predicted sun protection effectiveness of various hat styles. *Photodermatology, Photoimmunology and Photomedicine, 34*, 330–337.
49. Religi, A., & Moccozet, L. (2019). Modelling for solar erythemal UV protection provided by human hair. *Applied Sciences, 9*(22), 4724. https://doi.org/10.3390/app9224724
50. Parisi, A. V., Turnbull, D. J., Downs, N., & Smith, D. (2012). Dosimetric investigation of the solar erythemal UV radiation protection provided by beards and moustaches. *Radiation Protection Dosimetry, 150*, 278–282.
51. Parrish, J.-A., Zaynoun, S., & Anderson, R. R. (1981). Cumulative effects of repeated subthreshold doses of ultraviolet radiation. *The Journal of Investigative Dermatology, 76*, 356–358.
52. Arbabi, L., Gange, R. W., & Parrish, J. A. (1983). Recovery of skin from a single suberythemal dose of ultraviolet radiation. *The Journal of Investigative Dermatology, 81*, 78–82.
53. Kollias, N., Stamatas, G. N., & Youn, J. I. (2001). Suppression of UVB-induced cutaneous erythema by a previous UVB exposure. *Photochemistry and Photobiology, 74*, 471–476.
54. Gambichler, T., & Schröpl, F. (1998). Changes of minimal erythema dose after water and salt water baths. *Photodermatology, Photoimmunology and Photomedicine, 14*, 109–111.
55. Schempp, C. M., Müller, K., Schulte-Mönting, J., Schöpf, E., & Simon, J. C. (1999). Salt water bathing prior to UVB irradiation leads to a decrease of the minimal erythema dose and an increased erythema index without affecting skin pigmentation. *Photochemistry and Photobiology, 69*, 341–344.
56. Moehrle, M., Koehle, W., Dietz, K., & Lischka, G. (2000). Reduction of minimal erythema dose by sweating. *Photodermatology, Photoimmunology and Photomedicine, 16*, 260–262.
57. Mech, M., & Koepke, P. (2003). Model for UV irradiance on arbitrarily oriented surfaces. *Theoretical and Applied Climatology, 77*, 151–158.
58. Hoeppe, P., Oppenrieder, A., Erianto, C., Koepke, P., Reuder, J., Seefeldner, M., & Nowak, D. (2004). Visualization of UV exposure

of the human body based on data from a scanning UV-measuring system. *International Journal of Biometeorology, 49*, 18–25.
59. Vernez, D., Milon, A., Francioli, L., Bulliard, J.-L., Vuilleumier, L., & Moccozet, L. (2011). A numeric model to simulate solar individual ultraviolet exposure. *Photochemistry and Photobiology, 87*, 721–728.